



Deposited via The University of Sheffield.

White Rose Research Online URL for this paper:

<https://eprints.whiterose.ac.uk/id/eprint/224078/>

Version: Published Version

Proceedings Paper:

Coimbra Goncalves, M.C., Alsters, R., Curtis, D. et al. (2024) Evolution of surface quality in micromilling Ti-6Al-4V alloy with increasing machined length. In: Meyer, D., Karpuschewski, B., Eich, M. and Hettig, M., (eds.) Procedia CIRP. 7th CIRP Conference on Surface Integrity, 15-17 May 2024, Bremen, Germany. Elsevier, pp. 221-226. ISSN: 2212-8271. EISSN: 2212-8271.

<https://doi.org/10.1016/j.procir.2024.05.040>

Reuse

This article is distributed under the terms of the Creative Commons Attribution-NonCommercial-NoDerivs (CC BY-NC-ND) licence. This licence only allows you to download this work and share it with others as long as you credit the authors, but you can't change the article in any way or use it commercially. More information and the full terms of the licence here: <https://creativecommons.org/licenses/>

Takedown

If you consider content in White Rose Research Online to be in breach of UK law, please notify us by emailing eprints@whiterose.ac.uk including the URL of the record and the reason for the withdrawal request.

7th CIRP Conference on Surface Integrity

Evolution of surface quality in micromilling Ti-6Al-4V alloy with increasing machined length

Maria Clara Coimbra Gonçalves^a, Rob Alsters^b, David Curtis^c, Rachid M'Saoubi^{d,e}, Hassan Ghadbeigi^a^aUniversity of Sheffield, Mechanical Engineering Department, Mappin Street, Sheffield, UK^bR&D Materials and Technology Development, Seco Tools AB, Zandterweg 14, 5973 RC Lottum, Netherlands^cAdvanced Manufacturing Research Centre, University of Sheffield, Rotherham S60 5TZ, UK^dR&D Materials and Technology Development, Seco Tools AB, 737 82, Fagersta, Sweden^eDivision of Production and Materials Engineering, Lund University, Ole Römers väg 1, 221 00, Lund, Sweden* Corresponding author. E-mail address: mccoimbragoncalves1@sheffield.ac.uk

Abstract

Micromilling is a subtractive manufacturing process that presents challenges due to scale effects and rapid tool wear. To understand the evolution of surface quality when increasing the machined length during the micromilling process, this study assessed the surface roughness, topography, and defects of slots micromilled on Ti-6Al-4V. For the experiments, 1 mm diameter flat end mills were employed, and the cutting parameters were varied using a full factorial design. Subsequently, the surface texture field parameter S_a was assessed every 20 mm, up until the machining length of 260 mm. The analysed results led to the conclusion that, for the adopted set of parameters and the machining length of up to 260 mm, surface roughness was not significantly correlated to the machined length in the micromilling process of Ti-6Al-4V, as the Pearson coefficient, obtained from the correlation analysis, was -0.052. However, the surface roughness was mainly influenced by feed rate (Pearson coefficient of 0.82), with higher feed rates leading to rougher surfaces (up to $S_a = 0.4 \mu\text{m}$) due to the tool load increase that causes wider feed marks on the surface. Regarding the feed marks, they were affected by the tool rotational frequency due to system vibration. Additionally, surface defects of adhered material, smearing, tearing and side flow were observed. For lower feeds, material adhesion was the main type of defect observed, while higher feed rates favoured the side flow phenomenon.

© 2024 The Authors. Published by Elsevier B.V.

This is an open access article under the CC BY-NC-ND license (<http://creativecommons.org/licenses/by-nc-nd/4.0/>)Peer-review under responsibility of the scientific committee of the 7th CIRP Conference on Surface Integrity.**Keywords:** micromilling; surface quality; tool wear

1. Introduction

Micromilling is a manufacturing process that is applied across industries to obtain precise features or components. It consists on the milling process performed using micromills up to 1 mm diameter [1]. This process has gained attention over the last years due to the tendency towards components miniaturisation [2, 3]. However, the application of micromilling in industry is limited by its inherent physical process issues, as scale effects and process stability [4]. For this reason, the need to conduct in-depth research analysing this process mechanics is frequently emphasised in literature [3, 4, 5, 6], especially re-

garding surface quality, as this feature directly impact the part functionality.

In this area, Balázs and Takács [7] investigated the influence of micromilling cutting parameters on the surface quality of hardened steels. The authors focused on analysing the variation of the surface roughness parameters R_a and R_z with feed per tooth and depth of cut, and they also considered the Fast Fourier Transform (FFT) of the roughness profile to address characteristic frequencies involved in the formation of the surface profile. They concluded that feed per tooth and depth of cut significantly influenced the surface roughness results. An interesting aspect observed by the authors is that the distance of the feed marks on the machined surface correlates to the feed per rotation value, not to the feed per tooth. Presuming that both cutting edges remove material in each rotation, this phenomena can be attributed to a possible axial run-out of the tool. Aurich

et al. [8] also analysed the influence of the cutting parameters on the micromilling process. However, the authors machined titanium grade 2 and brass (CuZn39Pb2) with a single edge tool of 50 μm diameter. The main goal of their research was to evaluate the influence of the tilt angle of the single edge microtool on the surface quality. They concluded that, unlike in macromachining, the tilt angle plays an important role on the surface roughness, burr formation and shape of the structures. Wang et al. [9] studied the surface topography when micromilling a Ti-6Al-4V alloy and the authors found that the main surface defects were caused by feed marks, metal debris, plastic side flow, smeared material, and grooves. In a recent work, Gonçalves et al. [10] made a comparative analyses of the micromilling process when machining the Ti-6Al-4V wrought alloy and the alloy manufactured by Laser Powder Bed Fusion (LPBF). Both surface roughness and burr formation were assessed by analysing the S_a parameter and burr area, respectively. A better surface quality was obtained when machining at higher speed (60 m/min) and lower tool diameter (0.5 mm), due to the increase in the material removal rate that lead to a smoother surface. On the other hand, in the experiments with lower material removal rate, higher burr formation was obtained.

Even though some research have been dedicated on analysing surface roughness, achieving high surface quality remains a challenge in micromilling due to the numerous underlying mechanisms involved. In order to contribute with the current knowledge on this topic, this work aims to analyse how the surface quality progresses with machined length. To do that, the surface quality of the micromilled slots is going to be assessed by measuring the surface roughness and analysing the surface topography of a Ti-6Al-4V alloy. The Ti-6Al-4V is a material widely applied in industry, including medical and aerospace, due to its light weight and high resistance [11]. These industries often require microfeatures in this and other hard-to-machine materials for precision applications [3, 4, 6].

2. Methodology

2.1. Tools and workpieces

The microtools used to perform the experiments were 1 mm diameter solid carbide flat end mills, with two flutes, manufactured by SECO Tools. For the experiments, uncoated and SIRON-A coated (code: JME562010G2R010.0Z2-SIRA) tools were used in order to observe the coating influence on the analysed results. The tools' cutting edge radius, wedge angle and nose radius were measured using an optical 3D measuring system (Alicona Infinite Focus). These respective features for the uncoated and coated tools, averaged out of eight measurements, are presented in Table 1.

For each experiment made, a new tool was used. To standardise the inaccuracies and mitigate vibrations caused by tool bending during the cutting process, the tools were clamped to the tool holders maintaining a 15 mm distance from the collet to the tool tip. In total, eight tools each paired with a unique tool holder were used. Once the tools were clamped, their quasi-

Table 1: Tool measurements obtained in Alicona.

| Parameter | Uncoated tool | Coated tool |
|---------------------------------------|------------------|------------------|
| Cutting edge radius [μm] | 5.72 \pm 0.43 | 8.70 \pm 0.62 |
| Wedge angle [$^\circ$] | 70.18 \pm 2.34 | 71.20 \pm 4.28 |
| Nose radius [μm] | 88.09 \pm 2.16 | 85.34 \pm 6.01 |

static tool runout was measured with a dial indicator mounted on a magnetic base. The tool runout remained below 6 μm for all the tools, and they were not removed from their respective tool holder until the end of the tests.

For the experiments, a hot-rolled Ti-6Al-4V alloy was selected as the workpiece material due to its widespread application in industries. The hardness of the samples is 352.4 \pm 28.4 HV1 averaged out of six measurements. Its chemical composition, as provided by the manufacture's data, is presented in Table 2. The mechanical properties acquired through prior in-house testing on this material are detailed in Table 3.

Table 2: Chemical composition of the Ti-6Al-4V alloy (% by weight).

| Ti | Al | V | Fe | O | C | N | Y |
|----------|------|------|------|------|--------|---------|--------|
| Balanced | 6.39 | 3.94 | 0.17 | 0.17 | < 0.01 | < 0.002 | < 0.01 |

Table 3: Mechanical properties of the Ti-6Al-4V alloy.

| Yield strength [MPa] | Young Modulus [GPa] | Ultimate Tensile Strength [MPa] | % Elongation |
|---------------------------------|--------------------------------|--|--------------|
| 900 | 113 | 1000 | 20 |

In order to highlight the microstructure of the samples they were ground and polished with colloidal silica 0.04-0.06 μm and analysed in the Scanning Electron Microscope (SEM). Figure 1 shows the images obtained from the SEM (improved in the imageJ software for visualisation purposes only) in the samples' three different planes, where RD, TD and ND stands for rolling direction, transverse direction and normal direction, respectively. As it can be seen, columnar grains are observed in the rolling direction, which is the direction that the cutting process was performed. In Figure 1, f_z and a_p represent the feed and depth of cut directions in the sample.

2.2. Design of experiments

To perform the experiments, a Rödgers RXP 300 Micromachining Centre with a maximum spindle speed of 50000 rpm was used (Figure 2). Rectangular Ti-6Al-4V samples measuring 30x20x10 mm were mounted on a fixture and slots of 20 mm length were made following the DoE presented in Table 4, until a machined length of 260 mm was achieved for each condition. To accomplish this, 13 samples were used, and in each one of them eight slots were manufactured, one for each condition presented in Table 4. A space of twice the tool diameter was

left in between each slot. Before conducting the experiments, a cleaning process was done with a 6 mm tool to ensure a flat surface. As it can be seen in Table 4, the feed per tooth was varied in values smaller, closer and larger than the cutting radius. This was done to observe the process outcomes in the ploughing, ploughing-shearing and shearing regions. In order to check the experiments repeatability, an additional experiment was made repeating the feed of 8 μm/tooth for both types of tool used. All other constant variables are specified in Table 4.

Table 4: Design of experiments.

| Experiment | Tool | f_z (μm/tooth) | Constants |
|------------|----------|------------------|--|
| C1 | Coated | 1 | <ul style="list-style-type: none"> $V_c = 140$ m/min (44600 rpm) $a_p = 0.2$ mm Tool $\phi = 1$ mm Workpiece: Ti-6Al-4V Coolant: Air |
| C2 | | 8 | |
| C3 | | 15 | |
| C4 | | 8 | |
| U1 | Uncoated | 1 | |
| U2 | | 8 | |
| U3 | | 15 | |
| U4 | | 8 | |

3. Results

3.1. Surface roughness analysis

The arithmetical mean height S_a of the machined slots was analysed in an area of $800 \times 800 \mu\text{m}$ at the middle of each slot, using a cutoff wavelength (λ_c) of $80 \mu\text{m}$. Figure 3 present the contour plot of the machined surfaces, and Figure 4a and Figure 4b present the S_a progression with the examined machined length for the coated and uncoated tools, respectively. The machined length does not play an important role on the surface roughness results, while higher feed per tooth leads to higher S_a results. To confirm this relation, the Pearson coefficients between the input parameters and the surface roughness results

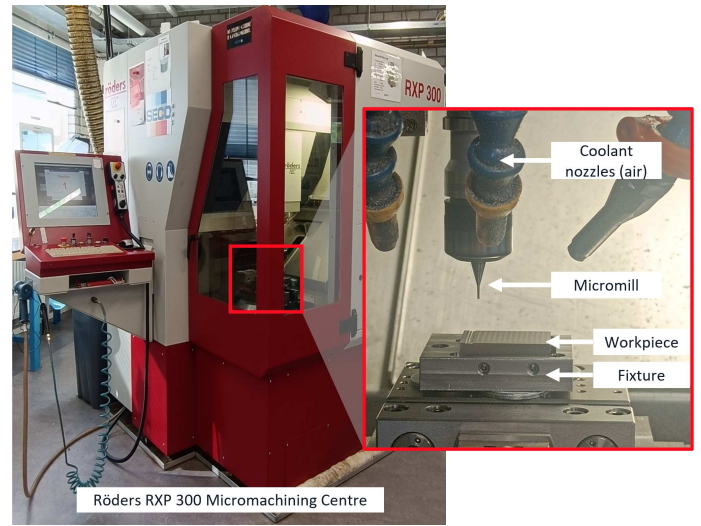


Fig. 2: Machine setup for the experimental trials.

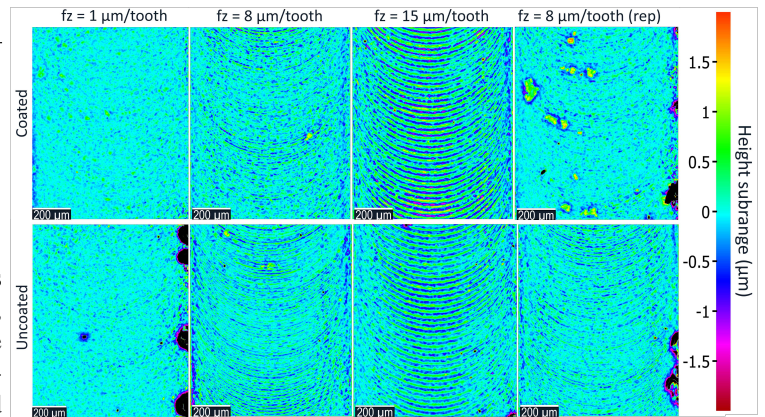


Fig. 3: Surfaces contour plot.

were calculated. The heat map of Figure 5 confirms that there is no correlation between the machined length and S_a results, while there is a strong correlation between the feed and the surface roughness. In addition, there was no correlation between the coating use and S_a results. As the feed increases, the tool load increases and the surface becomes rougher, mainly due to the feed marks left on the surface.

3.2. Surface topography analysis

To further analyse the feed marks left on the surface, their behaviour were analysed by acquiring the roughness profile in the middle of each slot and performing a fast Fourier transform (FFT) in this profile data to obtain the frequencies within it. The roughness profile for each slot were acquired in a profile length of 1 mm and using a cutoff wavelength (λ_c) of $80 \mu\text{m}$. The FFT analyses obtained are presented in Figures 6a and 6b for the coated and uncoated tools, respectively. Initially, it is possible to see that only the experiments made with the feed of $15 \mu\text{m}/\text{tooth}$ shows a distinctive peak around the spindle speed frequency, calculated as shown in Eq. 1. The experiments made

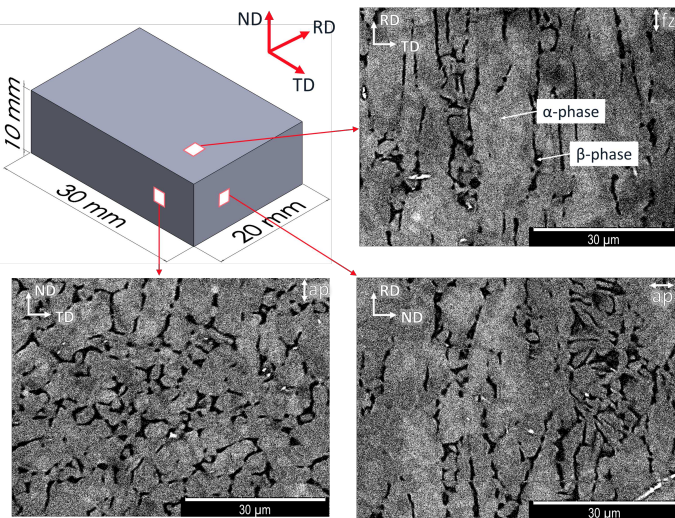
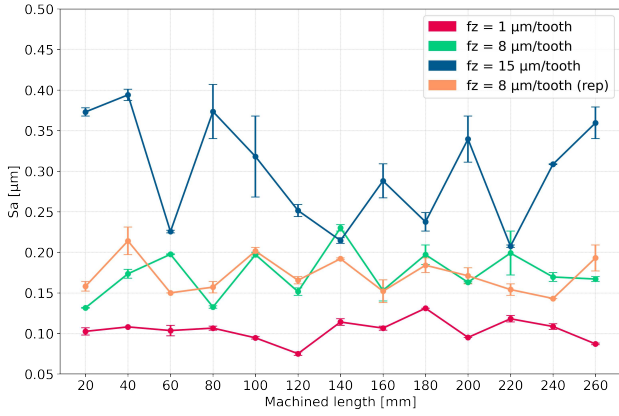
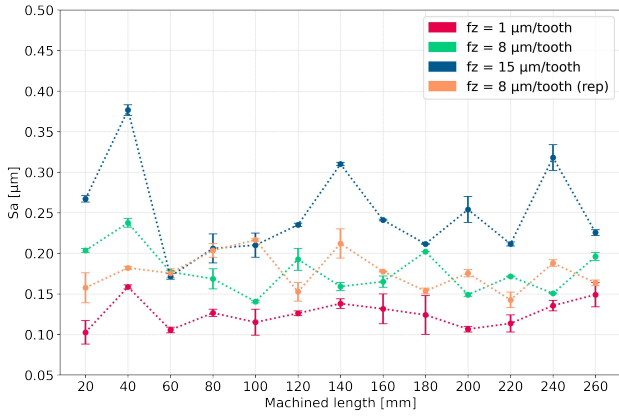


Fig. 1: Workpiece geometry and microstructure.

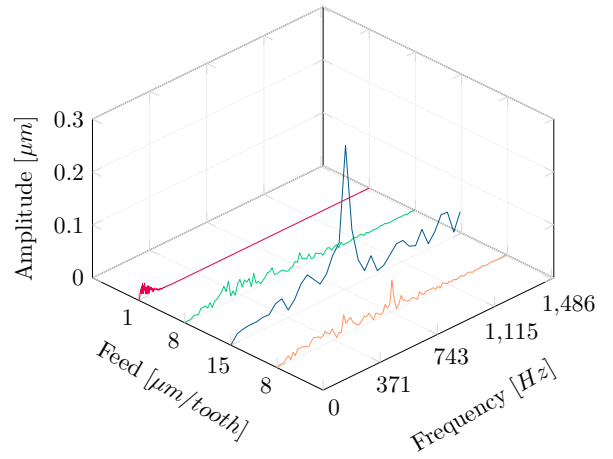


(a) Coated tools

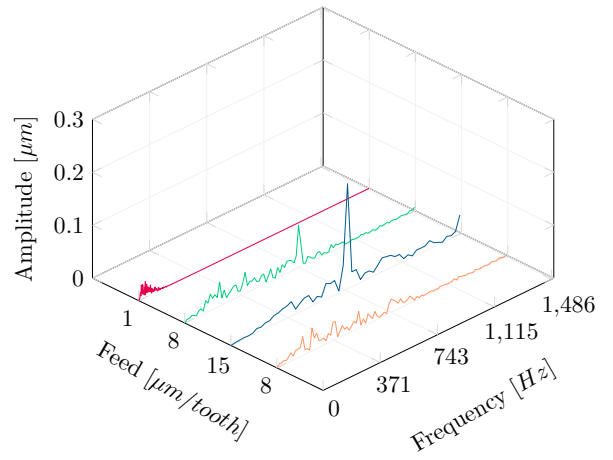


(b) Uncoated tools

Fig. 4: S_a variation with machined length for different feed rates using coated and uncoated tools



(a) Coated tools



(b) Uncoated tools

Fig. 6: Fast Fourier Transform plot for different feed rates using coated and uncoated tools

left on the surface are more visible for higher feed rates, as the tool load increases in this case (Figure 7). The material left causing the feed marks on the surface is also known as residual area [12], and it is caused due to a tool clearance angle different than zero and it is shaped by the tool nose radius, as illustrated in Figure 7. For lower feeds, as the surface is smoother, it is hard to obtain the frequency related to the cutting process, because the smearing and chips left on the surface will randomly affect the roughness profile data. The feed marks visibility can be observed in Figure 8.

$$f_{process} = \frac{N}{60} = \frac{44600}{60} Hz \rightarrow f_{process} = 743.33 Hz \quad (1)$$

It was expected that, as the tools have two teeth, the frequency of the feed marks should be twice the spindle speed frequency, as when a tooth is cutting the material it leaves a mark on the surface. However, when analysing the FFT results obtained in Figures 6a and 6b, it is possible to observe that the feed marks frequencies were related to the the feed per rotation value, not the feed per tooth, as also observed by Balázs and

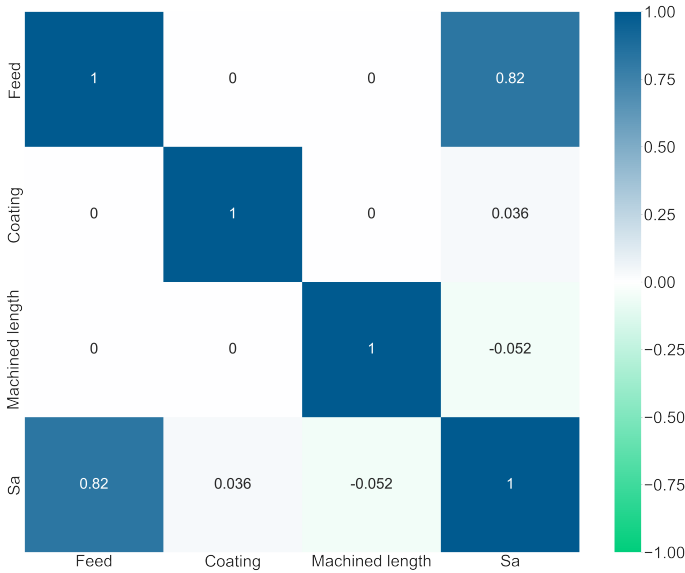


Fig. 5: Correlation analysis between the machining parameters and S_a

using the feed of $8 \mu\text{m/tooth}$ can show a moderate peak in this same frequency, while the $1 \mu\text{m/tooth}$ feed does not show frequencies in this range. This is due to the fact that the feed marks

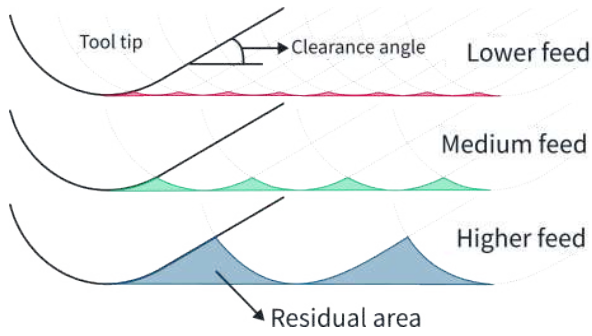


Fig. 7: Illustration of feed impact on feed marks

Takács [7]. When observing the tool wear images, both teeth present the same level of damage, what leads to the conclusion that both teeth were active when cutting the material. In Balázs and Takács [7] work, the authors attributed this behaviour to a possible axial tool run-out or size effects. However, in the present work, as the feed marks are precisely double the values of the feed per tooth, it is unlikely that they are due to tool run-out, as in this case, the feed marks should be the feed per tooth plus a tool run-out value. Since the values are related to the feed per rotation, the vibration of the system in this frequency can be the factor affecting the feed marks and, as a consequence, affecting the cutting process and actual feed value. To assure the FFT analyses were right, the feed marks distance were also measured, and they are about the same as the feed per rotation (Figure 8).

In summary, the surface roughness was mainly influenced by the feed marks left on the surface, leading to a rougher surface for higher feeds. However, no correlation was found between the surface roughness and the machined length, which can be observed from Figures 4 and 5.

3.3. Surface defects analysis

By analysing the machined slots, small defects such as adhered material, side flow, smearing and tearing were observed on the surfaces generated (Figure 9). The surface defects ob-

served were similar for the slots made using the coated and the uncoated tools. The adhered material is caused by the built-up edge unstable formation during the cutting process, which detaches from the tool tip and adheres to the machined surface [13]. This phenomenon appeared more frequently when using the lowest feed rate. The side flow phenomenon was mainly observed for the medium and high feed rates. This occurs as a result of the material softening under the high temperatures and pressures, achieved during the shearing process at higher feed rates, which results in the material being extruded by the tool, producing side flow [13]. In literature, smearing is also reported to occur due to the material being extruded between minor flank face and the machined surface [7, 9, 14]. Tearing on the surface can occur when small particles from the tool substrate or tool coating detach as the tool wears and rub against the surface, which leads to tearing surface [15].

4. Conclusions

This article focused on analysing the surface quality as the machined length progresses during the micromilling process of a Ti-6Al-4V alloy. The main findings of this research can be described as follows:

- No correlation between the machined length and surface roughness was observed for the set of parameters applied and up to the machined length of 260 mm with the correlation analysis resulting in a Pearson coefficient of -0.052.
- There was a strong positive correlation between the feed rate and S_a results (Pearson coefficient of 0.82). Thus, higher feed per tooth led to higher surface roughness (up to $S_a = 0.4 \mu\text{m}$), due an increase in the tool load.
- The surface features/defects were similar for the slots manufactured with the coated and uncoated tools, and no correlation was found between the S_a results and tool coating.

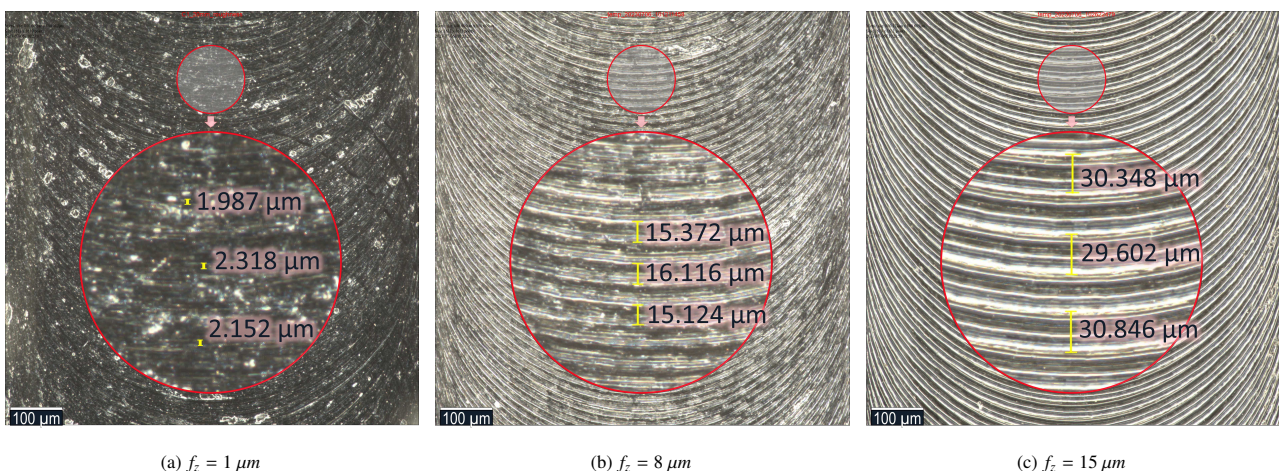


Fig. 8: Distance measurements between feed marks residual areas for the three different feed per tooth tested

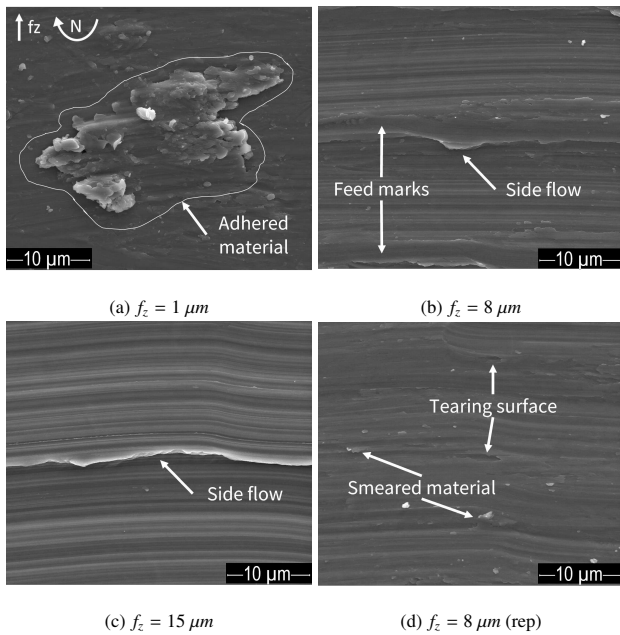


Fig. 9: Micrographs captured near the machined length of 260 mm (coated tool) showing the surface defects on the machined slots

- The feed marks on the surface are affected by the tool rotational frequency, which can be addressed to the system vibration.
- When analysing the machined surface, defects such as material adhesion, side flow, smeared material and tearing surface were observed.
- Lower feed led to more material adhered on the machined surface. While the increase in feed favoured the side flow phenomenon.

Acknowledgements

This study was financially supported under the grants of the Engineering and Physical Sciences Research Council (EPSRC) Doctoral Training Partnership Case Conversion with Seco Tools. Additionally, the authors would like to thank the R&D department at Seco Tools for all the support provided during the experimental trials.

References

- [1] M.A. Câmara, J.C. Campos Rubio, A.M. Abrão, and J.P. Davim. State of the art on micromilling of materials, a review. *Journal of Materials Science & Technology*, 28(8):673–685, 2012. ISSN 1005-0302. doi: 10.1016/S1005-0302(12)60115-7.
- [2] L.L. Alhadeff, M.B. Marshall, D.T. Curtis, and T. Slatter. Protocol for tool wear measurement in micro-milling. *Wear*, 420-421:54–67, 2019. ISSN 0043-1648. doi: 10.1016/j.wear.2018.11.018.
- [3] E. Kuram and B. Ozcelik. Optimization of machining parameters during micro-milling of Ti6Al4V titanium alloy and Inconel 718 materials using Taguchi method. *Proceedings of the Institution of Mechanical Engineers, Part B: Journal of Engineering Manufacture*, 231(2):228–242, 2015. doi: 10.1177/0954405415572662.

- [4] L. O’Toole, C. Kang, and F. Fang. Precision micro-milling process: state of the art. *Advances in Manufacturing*, 9, 10 2020. doi: 10.1007/s40436-020-00323-0.
- [5] S.H.I. Jaffery, M. Khan, L. Ali, and P.T. Mativenga. Statistical analysis of process parameters in micromachining off Ti-6Al-4V alloy. *Proceedings of the Institution of Mechanical Engineers, Part B: Journal of Engineering Manufacture*, 230(6):1–18, 2015. doi: 10.1177/0954405414564409.
- [6] M.C. Gomes, A.G. dos Santos, D. de Oliveira, G.V. Figueiredo, K.S.B. Ribeiro, G.A.B. de Los Rios, M.B. da Silva, R.T. Coelho, and W.N.P. Hung. Micro-machining of additively manufactured metals: a review. *The International Journal of Advanced Manufacturing Technology*, 118:2059–2078, 2022. doi: 10.1007/s00170-021-08112-0.
- [7] B.Z. Balázs and M. Takács. Experimental investigation of the influence of cutting parameters on surface quality and on the special characteristics of micro-milled surfaces of hardened steels. *Proceedings of the Institution of Mechanical Engineers, Part C: Journal of Mechanical Engineering Science*, 235(23):6996–7008, 2021. doi: 10.1177/09544062211013064.
- [8] J.C. Aurich, M. Bohley, I.G. Reichenbach, and B. Kirsch. Surface quality in micro milling: Influences of spindle and cutting parameters. *CIRP Annals*, 66(1):101–104, 2017. ISSN 0007-8506. doi: 10.1016/j.cirp.2017.04.029.
- [9] Y. Wang, B. Zou, J. Wang, Y. Wu, and C. Huang. Effect of the progressive tool wear on surface topography and chip formation in micro-milling of Ti-6Al-4V using Ti(C7N3)-based cermet micro-mill. *Tribology International*, 141:105900, 2020. ISSN 0301-679X. doi: 10.1016/j.triboint.2019.105900.
- [10] M.C.C. Gonçalves, M.C. Gomes, R.L. Stoeterau, G.F. Batalha, and M.B. da Silva. Influence of the material manufacturing process on micromilling Ti6Al4V alloy. *International Journal of Advanced Manufacturing Technology*, 2023. doi: 10.1007/s00170-023-12215-1.
- [11] G. Lütjering and J.C. Williams. *Titanium*. Springer, 2007.
- [12] X. Wu, Z. Chen, W. Ke, F. Jiang, M. Zhao, L. Li, J. Shen, and L. Zhu. Investigation on surface quality in micro milling of additive manufactured Ti6Al4V titanium alloy. *Journal of Manufacturing Processes*, 101:446–457, 2023. ISSN 1526-6125. doi: 10.1016/j.jmapro.2023.05.110.
- [13] X. Li, Z. Liu, and X. Liang. Tool wear, surface topography, and multi-objective optimization of cutting parameters during machining AISI 304 austenitic stainless steel flange. *Metals*, 9(9), 2019. ISSN 2075-4701. doi: 10.3390/met9090972.
- [14] R.S. Pawade, Suhas S. Joshi, P.K. Brahmkar, and M. Rahman. An investigation of cutting forces and surface damage in high-speed turning of Inconel 718. *Journal of Materials Processing Technology*, 192-193:139–146, 2007. ISSN 0924-0136. doi: https://doi.org/10.1016/j.jmatprotec.2007.04.049. The Seventh Asia Pacific Conference on Materials Processing (7th APCMP 2006).
- [15] M.R. Hassan, M. Mehrpouya, and S. Dawood. Review of the machining difficulties of nickel-titanium based shape memory alloys. *Applied Mechanics and Materials*, 564:533–537, 06 2014. doi: 10.4028/www.scientific.net/AMM.564.533.